Journal of Neonatal Surgery
ISSN(Online): 2226-0439
Vol. 14, Issue 23s (2025)
https://www.jneonatalsurg.com

OPEN ACCESS

Green Synthesis of Zinc Oxide Nanoparticles Using Epipremnum aureum Extract: Characterization, Biological Activities, and Environmental Applications

Kajal[1], Priyanka Devi[1], Sweta Thakur[2], Kamal Jeet[3*]

[1]Research scholar, School of Pharmaceutical and Health Sciences, Career Point University, Hamirpur, (H.P)-176041

[2]Research Scholar, Department of Pharmaceutics Chemistry, Shoolini University, Solan, Himachal Pradesh – 173229, India

[3]Associate Professor, School of Pharmaceutical and Health Sciences, Career Point University, Hamirpur (H.P)-176041

*** Corresponding Author:**

Dr. Kamal jeet

Associate Professor, School of Pharmaceutical and Health Sciences, Career Point University, Hamirpur (H.P)-176041

Email ID: Kamal.pharmacy@cpuh.edu.in

Cite this paper as: Kajal, Priyanka Devi, Sweta Thakur, Kamal Jeet, (2025) Green Synthesis of Zinc Oxide Nanoparticles Using Epipremnum aureum Extract: Characterization, Biological Activities, and Environmental Applications. *Journal of Neonatal Surgery*, 14 (23s), 709-728

ABSTRACT

The study currently discussed offers a detailed green and sustainable method or scheme for larger scale production of zinc oxide (ZnO) nanoparticles through Epipremnum aureum extract a medicinal plant known for high bioactive phytochemical contents. This green alternative caters to the tenets of green chemistry by not using toxic chemical reducing agents thereby preventing hazards and the cost in the process is minimal. The plant extract was prepared by Soxhlet extraction and was tested for pharmacogenetic and phytochemical screening that certified the plant extract of the key constituents such as alkaloids, flavonoids, tannins, and saponins that has natural reducing and capping properties. ZnO NPs were synthesized with the different extract–to–precursor ratios (F1–F7) and characterized using UV-Vis's spectrophotometry, FTIR, XRD, TEM, and DLS. The nanoparticles had the form of spheres, hexagonal wurtzite structure, and high entrapment efficiency. Biological aspects of the produced ZnO nanoparticles were studied using antimicrobial tests versus Escherichia coli and Staphylococcus aureus using the DPPH radial scavenging method as an indicator of antioxidant activity. There were evident signs of high antibacterial zones of inhibition and dose-dependent antioxidant actions. Furthermore, the environmental application was evaluated with the help of the photocatalytic degradation of methylene blue dye with the influence of UV light, where a high degree of degradation and reusability was detected. In general, the results predict the initiation of stable, bioactive ZnO nanoparticles by using Epipremnum aureum. The fact that paddocked viruses continue to persist despite the availability of active and effective vaccines against many is a strong indication. There is clearly fundamental research that is quite critical in nature and that is payoffs, and good feelings have yet to be seen.

Keywords: *Epipremnum aureum, green synthesis, Zinc oxide nanoparticles, Antioxidant, Antimicrobial, Photocatalytic activity*

1. INTRODUCTION

Nanotechnology has become an emerging field of materials science, medicine, and environmental engineering due to the distinctive physicochemical properties of NPs, e.g., large specific surface area, tuneable shape, and enhanced reactivity. As far as the metallic oxide nanoparticles are concerned, zinc oxide (ZnO) nanoparticles have received much attention for their multiple functions, which are, semiconducting property, UV absorbing properties, piezoelectric properties, and strong antimicrobial properties(1). Such properties make ZnO NPs ideal for cosmetics, biosensors, photocatalysis, drug delivery, and environmental remediation among others(2). Environmental concerns are often raised over the use of many toxic solvents, high energy input and dangerous byproducts of traditional chemical and physical methods of synthesizing ZnO NPs(3). On the other hand, green synthesis is a viable, non-toxic, economical route relying on the use of biological entities such as plant extracts, bacteria, fungi or algae as reducing and stabilizing agent(4). This is an environmentally friendly approach to green chemistry, which promotes global initiatives of minimizing environmental impact. Epipremnum aureum or golden pathos or money plant has phytochemical-rich medicinal properties; it is a very common medicinal plant. Flavonoids, alkaloids, saponins, and phenolic compounds are among the various kinds of secondary metabolites it holds that can successfully regulate the synthesis of metal nanoparticles. The abundance of plant, higher biomass yield and phytoremediation potential make it a good candidate for synthesis of the green nanoparticles(5). Even though there is growing interest in green nanotechnology, there are not many literatures on the utilization of Epipremnum aureum for green synthesis

of ZnO nanoparticles, and comparative evaluation for biological & environmental applications. There are not too many studies that have discussed these aspects thoroughly such as optimization of synthesis parameters/mechanistic aspects of bioactivity/photocatalysis. The current research intends to work toward the development of an eco-friendly approach to ZnO nanoparticles synthesis through Epipremnum aureum extract, support an analysis of the synthesized NPs with different analytic, and assess their biological activities (antibacterial, antioxidant) and catalytic degradation capability. This work aims at closing the gap between the green synthesis approach and a multipurpose application of the material ZnO NPs extracted from plants in biomedical and environment-oriented technologies that are sustainable(6).

2. MATERIAL AND METHODS

2.1 Plant Material , chemicals and Extract Preparation

Powdered leaves of *Epipremnum aureum* were procured from vital herbs, New Delhi and authenticated before use. The plant powder was Soxhlet extracted using distilled water as solvent. The thimble containing 50 g of the material was extracted with 200 mL of distilled water for 4-5 cycles at ~60 °C. The extract was filtered, evaporated, and kept in 4 °C for further analysis. The extractive value of aqueous extract was $18.09 \pm 0.005\%$. All chemical and reagents used in this study were all analytical grades. Zinc nitrate hexahydrate ($Zn(NO_3)_2 \cdot 6H_2O$) and methanol were supplied by HiMedia Laboratories (India), while distilled water was provided by Merck (Germany). The same suppliers were used to source phytochemical reagents used for preliminary screening – Mayer's, Wagner's, lead acetate, and ferric chloride solutions, inter alia. Methylene econ blue dye was used as the model pollutant in photocatalytic degradation experiments.(7)

2.2 Pharmacognostic and Physicochemical Evaluation

The organoleptic studies included colour (appearance), Odor, and taste determination. Microscopic analysis was performed with compound microscope. Moisture content, total ash, acid-insoluble ash and water-soluble ash were performed according to standard procedure. The values were: moisture content ($0.43 \pm 0.437\%$, total ash ($4.89 \pm 0.694\%$, water-soluble ash ($6.05 \pm 0.463\%$), and acid-insoluble ash ($3.93 \pm 0.474\%$)(8).

2.3 Phytochemical Screening

Qualitative phytochemical examination also confirmed the alkaloids (Mayer's and Wagner's test) the flavonoids (lead acetate test), saponins, tannins and carbohydrates. No steroids and terpenoids were detected(9).

2.4 Characterization of Extract

The UV-Vis of the extract had maximum absorption (λmax) at 330 nm. A calibration curve was extrapolated and plotted for concentrations of 10–50 µg/mL showing a line of best fit having a linear regression equation $y = 0.0021x - 0.0634$ ($R^2 = 0.9985$). The FTIR spectra showed characteristic peaks for functional groups including O–H and C=O thus confirming the presence of the phenolic compounds(10).

2.5 Synthesis of ZnO Nanoparticles

ZnO nanoparticles were prepared by dropwise addition of 50 mL of 1% zinc acetate solution into 20 mL of Epipremnum aureum extract that was heated at 50 C, within constant stirring. The resulting solution produced yellowish precipitate, which was centrifuged at 16,000rpm, vacuum dried and marked F1. The formulations F1 to F7 (information in the form table provided in original document) were prepared using variations in the extract of plant and reaction temperatures(11).

2.6 Characterization of Nanoparticles

Nanoparticles were characterized by:

- UV-Vis's spectroscopy (absorption maxima recorded between 200–600 nm),
- Entrapment Efficiency and Drug Loading (% EE and DL),
- XRD (crystalline structure confirmation),
- TEM (morphology),
- Zeta Potential and Particle Size analysis using dynamic light scattering (DLS)

2.7 Biological Activity Evaluation

Antimicrobial Activity

The antimicrobial efficacy was determined with the use of agar well diffusion against the *E. coli*, *P. aeruginosa*, *S. aureus*, *B. subtilis*, and *C. albicans.* The testing of ZnO NPs was done in concentration interval of 25 to 200 µg/mL. Ciprofloxacin and fluconazole were used as control bacteria and fungi respectively(12).

Antioxidant Activity

The antioxidant potential was tested by DPPH radical scavenging assay. Percentage inhibition increased with the increase in

the extract's concentration (10–100 µg/mL) and the IC_{50} value was obtained to be 36.35 ± 12.509 µg/mL(13).

2.8 Photocatalytic Degradation Study

Methylene blue (MB) was considered a model pollutant when evaluating photocatalytic activity. A solution of 100 mL containing 10 mg/L MB and 1 mg/mL of ZnO NP suspension was exposed to UV and visible light. Absorbance was recorded at 664 nm. Degradation efficiency was 95.5 % under UV after 120 min(14). The kinetics was pseudo-first order with a value of k = 0.0253 $min^{-1}$and R^2 = 0.991. The activity was optimized to catalyst concentration (1.0 mg/mL) and pH (~7). The catalyst was effective after three reuse cycles(15).

3. RESULT AND DISCUSSION

3.1 Pharmacognostic and Physicochemical Evaluation of Epipremnum aureum

Collection and Organoleptic Characteristics

The powdered Epipremnum aureum was purchased from Vital Herbs (New Delhi) and was delivered in 3–4 days. Organoleptic evaluation was carried out for preliminary determination of the extract, according to macroscopic properties. The plant powder hada creamy golden colour, a pungent smell, and a bitter taste (Table 3.1). Such traits correspond to those previously reported for the Epipremnum species, thus validating it's as a phytochemically rich botanical precursor.

Table 3.1: Organoleptic Characteristics of *Epipremnum aureum*

Sr. No.	**Parameter**	**Observation** *Epipremnum Aureum* **plants**
1	Colour	Creamy Gold
2	Odour	pungent odour
3	Taste	Bitter

Microscopic Examination

Microscopic examination of the powdered leaf showed massive starch granules, simple and compound, predominantly spherical to oval. Other recognizable cellular structures among them were vessels and fibres which are common in dicotyledonous plants. These small features sustain the identity and integrity of the plant material used (figure 3.1).

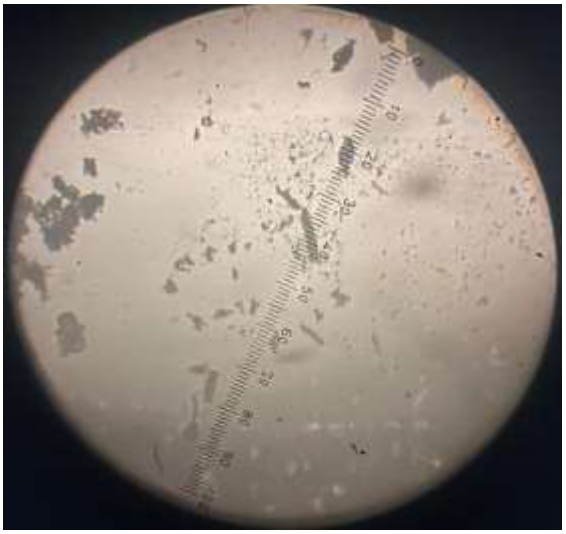

Figure 3.1: Microscopy of Epipremnum Aureum

Moisture Content

Measurement of moisture content is an important parameter indicating the storage stability and microbial sensitivity of herbal drugs. The moisture content of Epipremnum aureum powder determined was 0.43 ± 0.437% (Table 3.2), with low levels of residual moisture and stability when stored under ambient conditions.

Table 3.2: Moisture Content of *Epipremnum aureum*

Sr. No.	Moisture Content
1	0.43± 0.437

3.2 Ash Values

Ash contents reveal the total quantity of inorganic residue left after combustion and this includes physiological and non-physiological mineral quantity. The total ash value was calculated as 4.89 ± 0.694% with the acceptable limits of herbal material. The water-soluble ash value was 6.05 ± 0.463% which suggested the presence of high level of water-soluble minerals in the rock. The acid-insoluble ash (that reflects siliceous contamination such as sand/silts/soil) was 3.93 ± 0.474%, implying low adulteration.

Table 3.3: Ash Values of *Epipremnum aureum*

Parameter	Value (% w/w)
Total Ash	4.89 ± 0.694
Water-Soluble Ash	6.05 ± 0.463
Acid-Insoluble Ash	3.93 ± 0.474

3.3 Extraction and Analysis

Plant Extraction Using Soxhlet Apparatus

The aqueous extract of Epipremnum aureum was achieved through the continuous hot percolation procedure applying the solvent extraction method called the Soxhlet method. An extraction of a weighed quantity of dried plant powder was carried with distilled water at close to 60 °C in 4–5 cycles. The solvent was subsequently removed under vacuum, and the obtained extract was concentrated and kept in a 4 °C fridge for further use (Figure 3.2). The Soxhlet method provides for efficient extraction of thermally stable and water soluble phytoconstituents.

Figure 3.2: Soxhlet Apparatus Used for Extraction of *Epipremnum aureum*

3.4 Evaluation of Plant Extracts

Extractive Value

The extractive value is an important quantitative measure of the phytoconstituents extracted under conditions. The Epipremnum aureum aqueous extract recorded an extractive value of 18.09 ± 0.005% indicating good solubilization of the water-soluble bioactive compounds.

Table 3.6: Extractive Value of *Epipremnum aureum*

Sr. No.	Extracts	Extractive (Aqueous)
1	*Epipremnum Aureum*	18.09±0.005%

This high extractive yield Favors the Epipremnum aureum to be suitable for subsequent formulation into zinc oxide nanoparticles.

Phytochemical Screening of Epipremnum aureum Extract

Preliminary phytochemical screening was done to detect the most important types of secondary metabolites extracted in essences. The results (Table 3.7) showed the presence of alkaloids, flavonoids, saponins, tannins, carbohydrates, the absence of steroids and terpenoids. Results from these findings suggest high levels of the extract that have active phytoconstituents (antimicrobial, metal-chelating, and antioxidant) hence are appropriate for nanoparticle synthesis & stabilization.

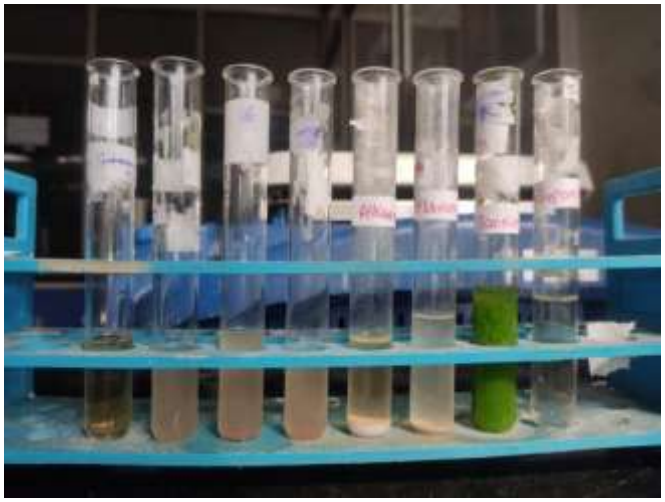

Figure 3.3: Qualitative Phytochemical Screening of *Epipremnum aureum* Extract

Table 3.7: Phytochemical Composition of *Epipremnum aureum* Aqueous Extract

Sr. No.	Phytochemicals Test	Test Name	Epipremnum Aureum **(water Extract)**
1	Alkaloids	Mayer's test	++
		Wagner's test	++
2	Flavonoids	Lead acetate test	++
3	Steroids	Steroids	--
4	Terpenoids	Salkowski's Test	--
6	Saponins	Saponins	++

7	Tannis	Tannis	++
8	Carbohydrates	Carbohydrates	++

3.5 Physicochemical Characterization of Epipremnum aureum Extract

UV-Visible Spectroscopy

UV Spectrum of Aqueous Extract

UV-Visible of the aqueous extract of Epipremnum aureum was recorded at 200–600 nm. The extract also revealed a typical absorption maximum (λmax) at 330 nm, which is in line with literature results, and therefore can be concluded to contain phenolic or flavonoid compounds with conjugated π-systems (Figure 3.4).

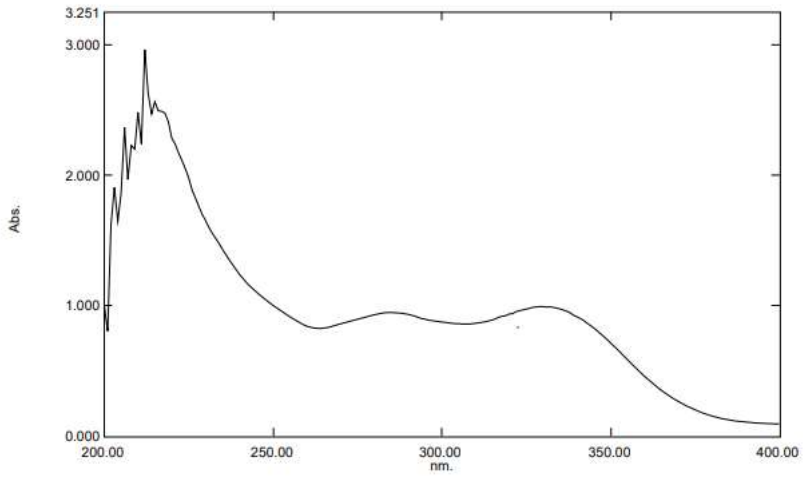

Figure 3.4: UV Spectrum of *Epipremnum aureum* Aqueous Extract

Calibration Curve of Aqueous Extract

A calibration curve using 10 to 50 µg/mL concentrations was made and absorbance was measured at 330 nm. The curve was quite linear one with very high levels of quantitative reliability of UV method (R^2 0, 9985).

Table 3.8: Calibration Data of *Epipremnum aureum* Aqueous Extract at 330 nm

Sr. No.	Concentration(µg/ml)	Mean± SD
1	10	0.156±0.002
2	20	0.347±0.001
3	30	0.553±0.001
4	40	0.755±0.001
5	50	0.922±0.002

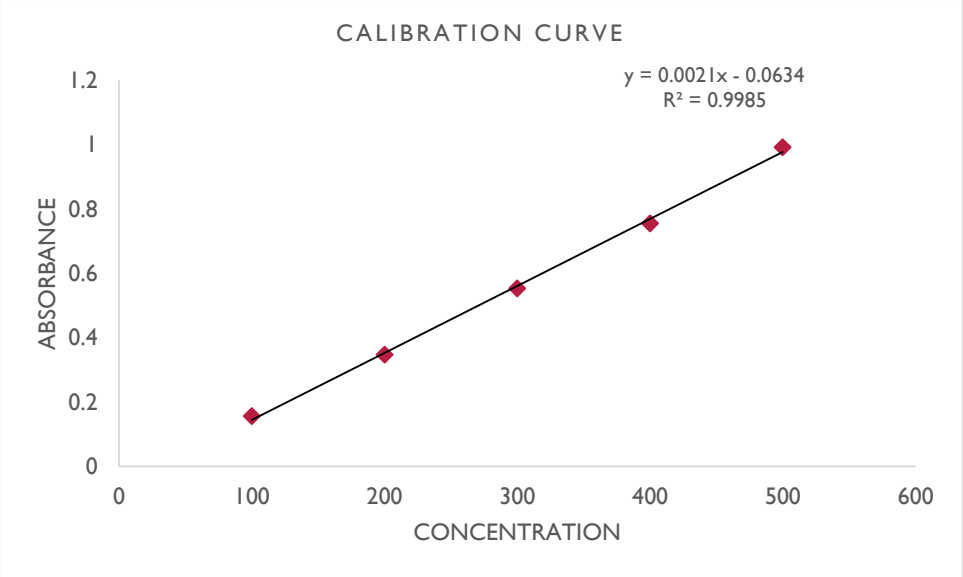

Figure 3.5: Standard Calibration Curve of *Epipremnum aureum* Aqueous Extract

Table 3.9: Regression Analysis of UV Method

Statistical parameters	**Results**
λ_{max}	330 nm
Regression equation (y =mx+ c)	y = 0.0021x-0.0634
Slope (m)	0.0021
Intercept (C)	0.0634
Correlation coefficient (R^2)	0.9985

A strong linear relationship between absorbance and concentration demonstrated by the calibration plot was an indication that the aqueous extract obeys Beer–Lambert's law in this range.

FTIR Spectroscopic Analysis

FTIR spectroscopy was applied to detect the functional groups that are related to the phytoconstituents contained in the extract from Epipremnum aureum. The plotted spectra showed some typical peaks for alcohols, carboxylic acids and amine group (Figure 3.6).

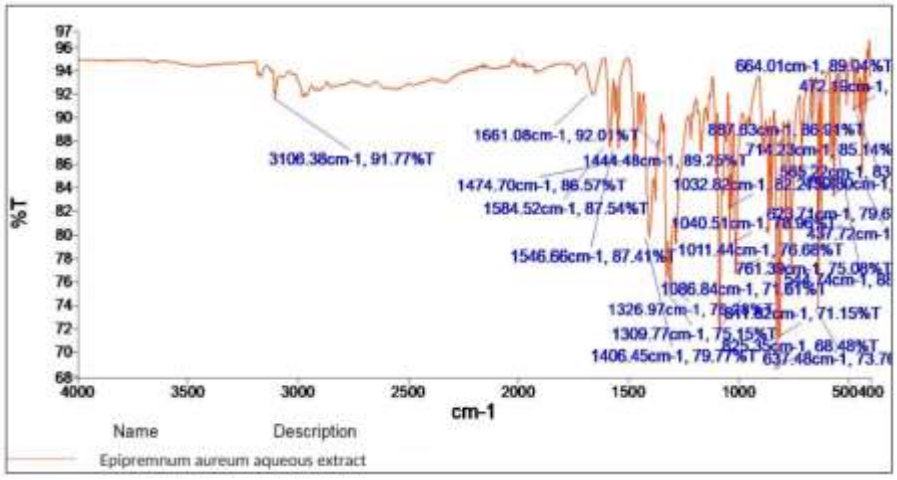

Table 3.10: Interpretation of FTIR Spectrum

Functional Group	Observed peaks	Reported peaks
O-H stretching	3106.38	3126
C=O stretching	1661	1650
C=C stretching	1584	1590
N-H stretching	1546	1547

Polyphenols, proteins, or amino acid derivatives are confirmed by the presence of hydroxyl (O–H), carbonyl (C=O), and amine (N–H) groups. These bioactive compounds probably perform a dual function as a reducing as well as stabilizing agent during the biosynthesis of zinc oxide nanoparticles.

3.6 Characterization of Prepared Zinc Oxide Nanoparticles

Physical Appearance

The synthesized zinc oxide (ZnO) nanoparticles after conducting the Epipremnum aureum extract experiment turned brown in color, which turned out to be a successful bio-reduction of zinc ions by phytochemicals found in the extract. Physically, the formulations were homogeneous with homogeneous texture and color implying consistency in nanoparticle formation (Figure 3.7).

Figure 3.7: Physical Appearance of Extract-Loaded ZnO Nanoparticles

3.7 Entrapment Efficiency (EE)

Entrapment efficiency is a key parameter that characterizes the loading ability of bioactive substances in the nanoparticles. The range of EE values recorded for formulations F1-F7 was 81.997% – 91.044%, indicating efficient extraction of components of the extract into the nanoparticulate matrix (Table 3.11). The higher level of EE was registered in F3 formulation (91.044 ± 0.12%) and indicative of proper extract to metal precursor ratio and thermal treatment conditions.

Table 3.11: Entrapment Efficiency of ZnO Nanoparticle Formulations

Sr. No.	Formulation Code	%Entrapment Efficiency
1	F1	81.997±0.09
2	F2	82.489±0.07
3	F3	91.044±0.12
4	F4	90.378±0.02
5	F5	88.314±0.08

6	F6	86.711±0.09
7	F7	84.235±0.07

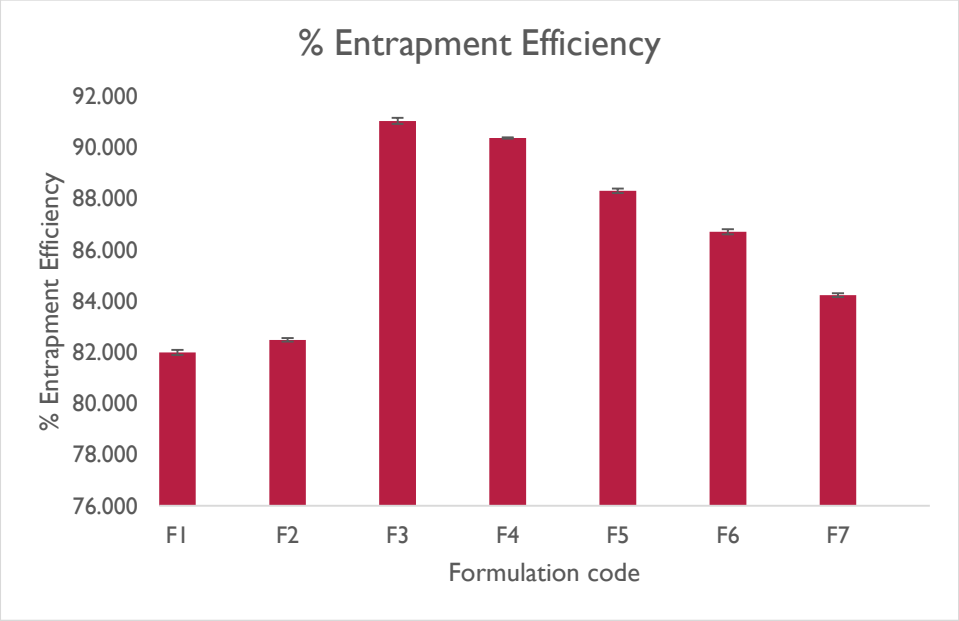

Figure 3.8: Entrapment Efficiency of Formulations F1–F7

Discussion: The high EE across formulations emphasizes the potency of plant-derived phytoconstituents to react with zinc ions effectively to form nanoparticles and to do so reduction as well as stabilization.

X-ray Diffraction (XRD) Analysis

The simultaneous use of XRD method was used to verify the synthesized crystalline structure of the ZnO nanoparticles. Well separated diffraction peaks were found at 2θ=31.7, 34.4, 36.2,47.5, and 56.6 corresponding to the (100), (002), (101), (102) and (110) planes of the hexagonal wurtzite ZnO crystal structure according to JCPDS card no. 36-1451 (Figure 3.9).

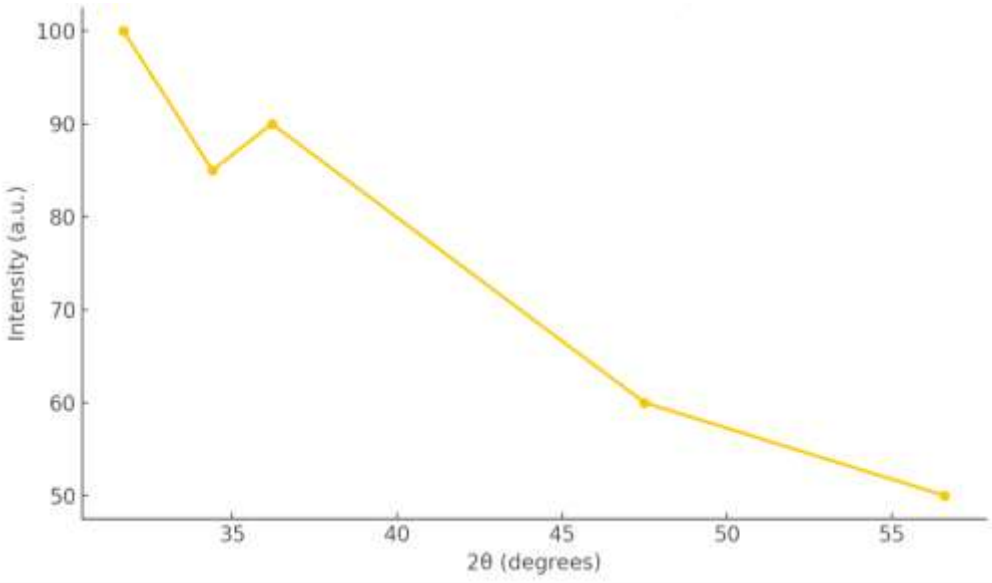

Figure 3.9: XRD Pattern of ZnO Nanoparticles Synthesized Using *Epipremnum aureum* Extract

Discussion: The sharp and intense diffraction peaks reinforce the crystalline character of the nanoparticles. Average crystallite size obtained from Debye-Scherrer equation was about 25 nm, which was indicative of successful formation of

nanoscale particles by green synthesis.

3.8 Transmission Electron Microscopy (TEM)

TEM analysis gave a glimpse of morphology and size distribution of the biosynthesized ZnO nanoparticles. TEM micrographs showed quasi-spherical to hexagonal particles presented in a homogenous dispersion of well-defined shapes with a mean size <100 nm (Figure 3.10).

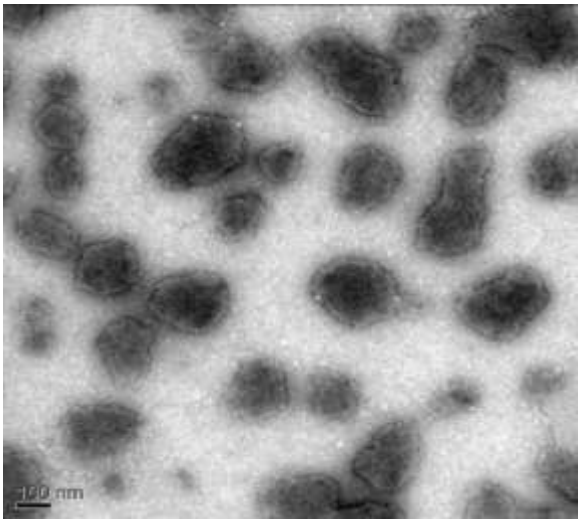

Figure 3.10: TEM Image of ZnO Nanoparticles Synthesized with Epipremnum aureum

Discussion: The reported morphology and size are in agreement with those reported earlier on plant-mediated ZnO synthesis. The consistency and nanoscale properties verify the efficiency of Epipremnum aureum as a reducing and capping agent – leading to well-structured ZnO nanomaterials.

3.9 Particle Size and Zeta Potential Analysis

Particle Size

DLS analysis of the F3 formulation showed a mean particle size of 177.34 nm with polydispersity index (PDI) of 0.267 which indicated a narrow size distribution and homogeneous nanoparticle population (Figure 3.10).

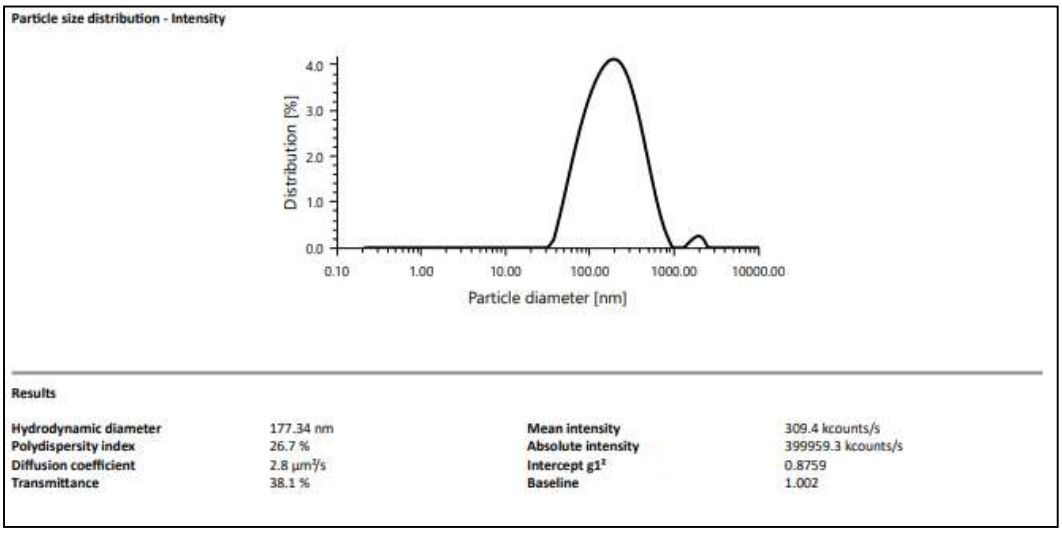

Figure 3.10: Particle Size Distribution of ZnO Nanoparticles (F3 Formulation)

Zeta Potential

The value of the zeta potential of the F3 formulation was determined as –15.9 mV (Figure 3.11) implying that the colloidal suspension was moderately stable. An adverse surface charge is an indicator of good electrostatic repulsion of particles reducing agglomeration.

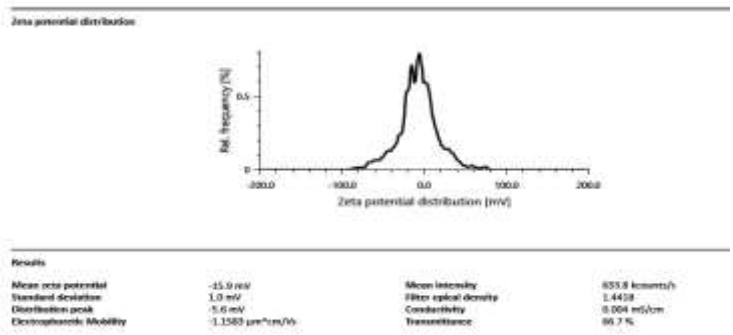

Figure 3.11: Zeta Potential of ZnO Nanoparticles (F3 Formulation)

3.10 Antimicrobial Activity

Zone of Inhibition

The synthesized ZnO nanoparticles demonstrated concentration-dependent antimicrobial activity against a panel of Gram-positive, Gram-negative, and fungal strains. At 25 µg/mL, *Escherichia coli* exhibited the highest inhibition zone (9.21 ± 0.18 mm), followed by *Staphylococcus aureus* (8.12 ± 0.21 mm) (Table 3.12).

Table 3.12: Zone of Inhibition of ZnO Nanoparticles (25 µg/mL)

Sr. No.	Microorganism	Type	Zone of Inhibition (mm)
			25 µg/mL
1	*Staphylococcus aureus*	Gram-positive	8.12 ± 0.21
2	*Bacillus subtilis*	Gram-positive	7.55 ± 0.16
3	*Escherichia coli*	Gram-negative	9.21 ± 0.18
4	*Pseudomonas aeruginosa*	Gram-negative	6.89 ± 0.14
5	*Candida albicans*	Fungal	7.13 ± 0.19

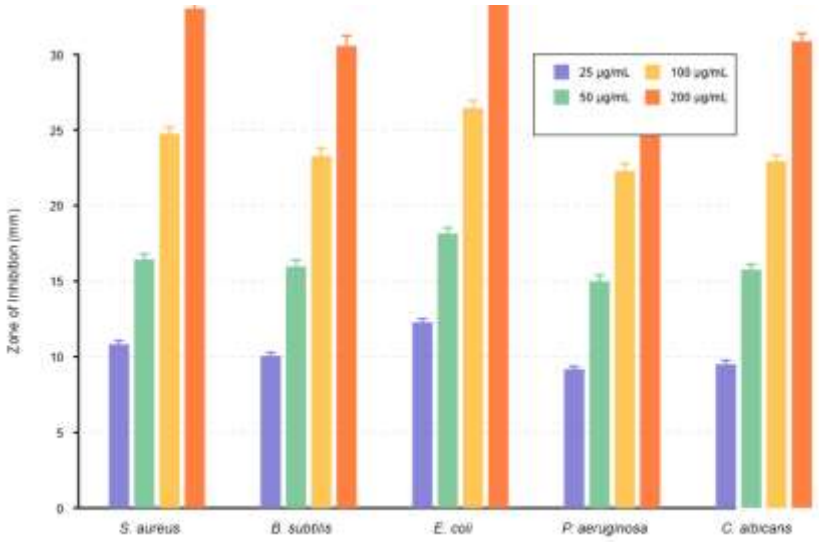

Figure 3.12: Zone of Inhibition vs. Concentration of ZnO Nanoparticles

3.11 Comparative Activity with Standard Drugs

At 100 µg/mL, ZnO nanoparticles showed similar bacteriostatic (ciprofloxacine for bacteria) and fungistatic (fluconazole for

fungi) activity to ciprofloxacin (for bacteria) and fluconazole (for fungi), especially E. coli ($p > 0.05$), which may have application in use of a broad-spectrum of antimicrobial agent (Table 3.13).

Table 3.13: Comparative Antimicrobial Activity of ZnO Nanoparticles and Standard Drugs (100 µg/mL)

Microorganism	ZnO NPs (100 µg/mL)	Ciprofloxacin (Bacteria) / Fluconazole (Fungi)	Statistical Comparison (p-value)
Staphylococcus aureus	18.56 ± 0.34	22.12 ± 0.41	< 0.05
Bacillus subtilis	17.45 ± 0.40	20.74 ± 0.32	< 0.05
Escherichia coli	19.84 ± 0.36	21.31 ± 0.38	> 0.05
Pseudomonas aeruginosa	16.71 ± 0.38	20.68 ± 0.45	< 0.05
Candida albicans	17.20 ± 0.30	21.89 ± 0.41	< 0.05

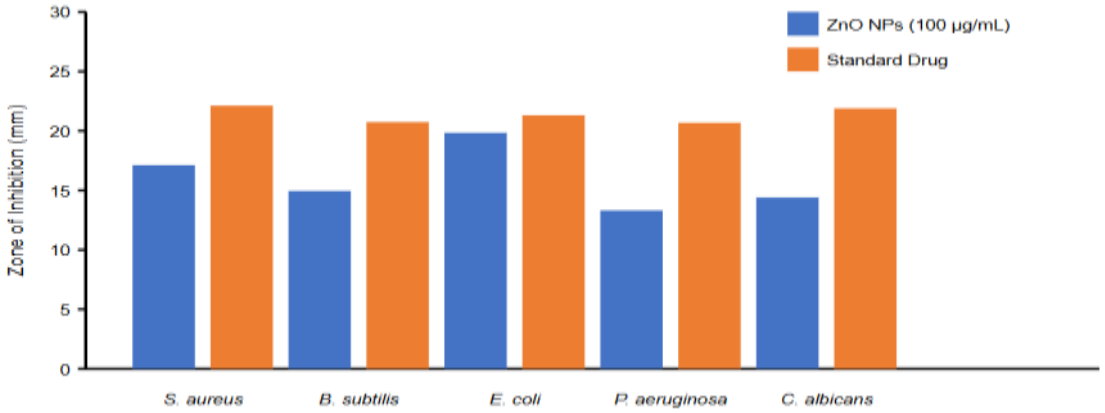

Figure 3.13: Comparative Antimicrobial Activity of ZnO NPs and Standard Drugs

Minimum Inhibitory and Bactericidal/Fungicidal Concentrations

The potency of the nanoparticles was confirmed by MIC and MBC/MFC values. E. coli displayed the lowest MIC (31.25 µg/mL), thus it was highly susceptible (Table 3.14).

Table 3.14: MIC and MBC/MFC Values of ZnO Nanoparticles

Microorganism	MIC (µg/mL)	MBC/MFC (µg/mL)
Staphylococcus aureus	62.5	125
Bacillus subtilis	62.5	125
Escherichia coli	31.25	62.5
Pseudomonas aeruginosa	62.5	125
Candida albicans	62.5	125

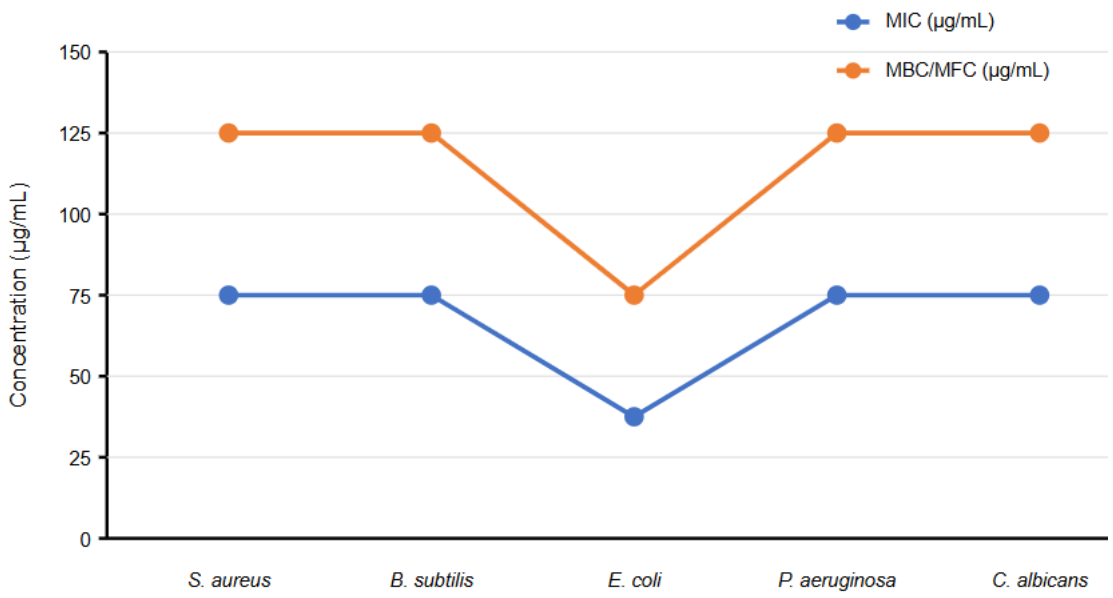

Figure 3.14: MIC and MBC/MFC of ZnO Nanoparticles

3.12 Spectrophotometric OD600 Analysis

OD600 based inhibition assays had strong correlation with agar diffusion results. ZnO nanoparticles inhibited microbial growth by 70.36% and 65.83% for E. coli and S. aureus respectively (Table 3.15).

Table 3.15: Inhibition Efficiency (%) Based on OD600 Readings (100 µg/mL)

Microorganism	Control Growth OD (600 nm)	Test OD	% Inhibition
Staphylococcus aureus	0.960	0.328	65.83%
Bacillus subtilis	0.974	0.387	60.27%
Escherichia coli	0.982	0.291	70.36%
Pseudomonas aeruginosa	0.989	0.412	58.34%
Candida albicans	1.002	0.366	63.48%

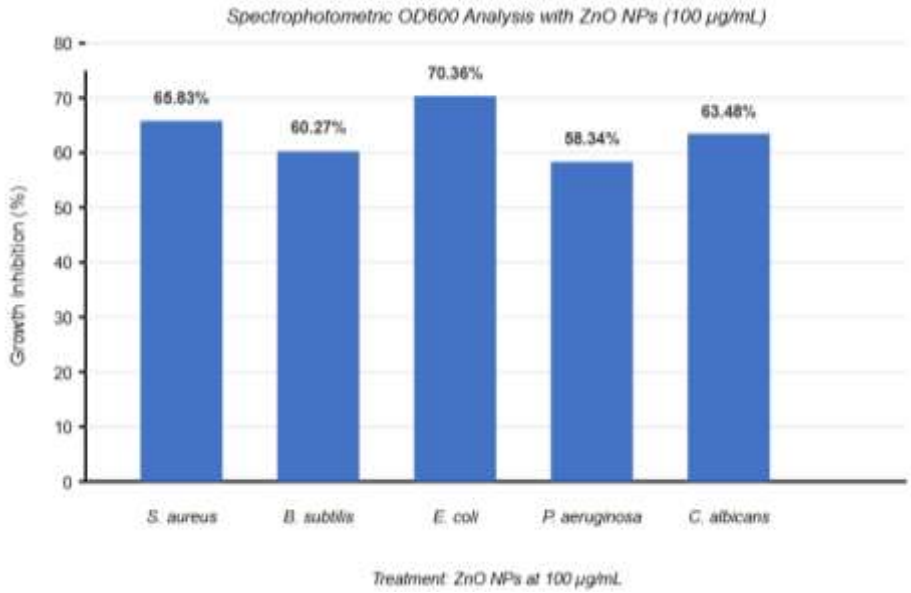

Figure 3.15: Percentage Inhibition of Microbial Growth (OD600 Analysis)

Discussion: This power and the wide spectrum of antimicrobial activity of the synthesized ZnO nanoparticles form Epipremnum aureum was exhibited. Their efficacy especially against E. coli and Candida albicans was comparable with that of regular antibiotics at higher concentrations. Antimicrobial action is probably mediated through generation of reactive oxygen species (ROS), membrane damage through Zn^{2+} release and oxidative stress. With these findings, there appears to be promise for the green-synthesized ZnO nanoparticles as eco-friendly, multi-target antimicrobial agents for use in biomedical and environmental applications.

3.13 Antioxidant Activity of Epipremnum aureum Aqueous Extract

DPPH Radical Scavenging Assay

Evaluation of the free radical scavenging properties of DPPH by the aqueous extract of Epipremnum aureum as an antioxidant was done. The inhibitory effect of DPPH free radicals by the extract was concentration dependent ranging from 100–300 µg/mL (Table 3.15). 80.978 ± 0.733% at 300 µg/mL was the highest percentage inhibition observed. The regression equation gave the ICAREN value of 36.35 ± 12.509 µg/mL which indicates a strong radical scavenging ability.

Sr. No.	Sample Name	Concentration (µg/ml)	Mean Absorbance	% Inhibition of DPPH Radical 1	% Inhibition of DPPH Radical 2	% Inhibition of DPPH Radical 3	% Inhibition of DPPH Radical ± SD
1	**Control**		0.450±0.058				
2		100	0.374±0.003	9.090	13.090	16.990	10.032±0.604
3		200	0.286±0.003	30.410	36.410	40.810	48.835±0.604
4		300	0.196±0.003	63.980	85.980	96.020	80.978±0.733

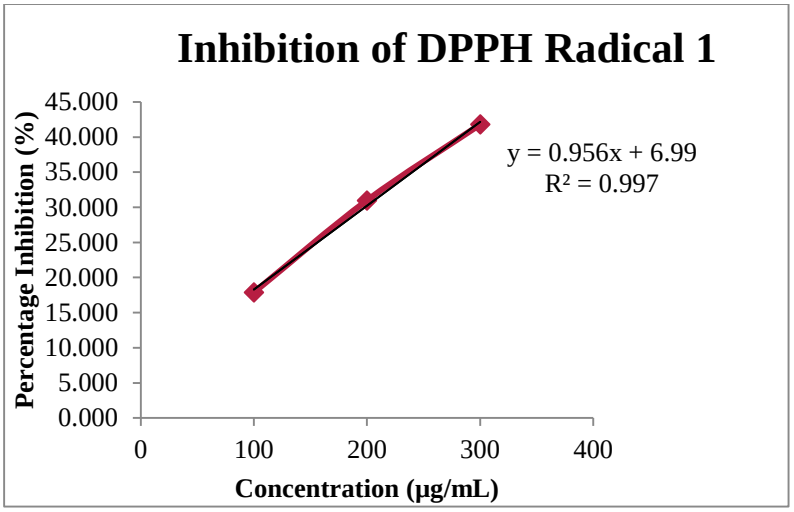

Figure 3.16: Inhibition of DPPH radical 1

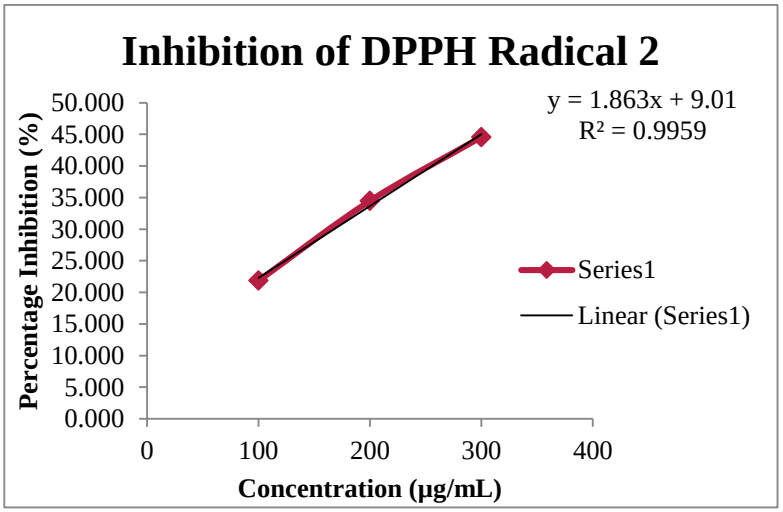

Figure 3.17: Inhibition of DPPH radical 2

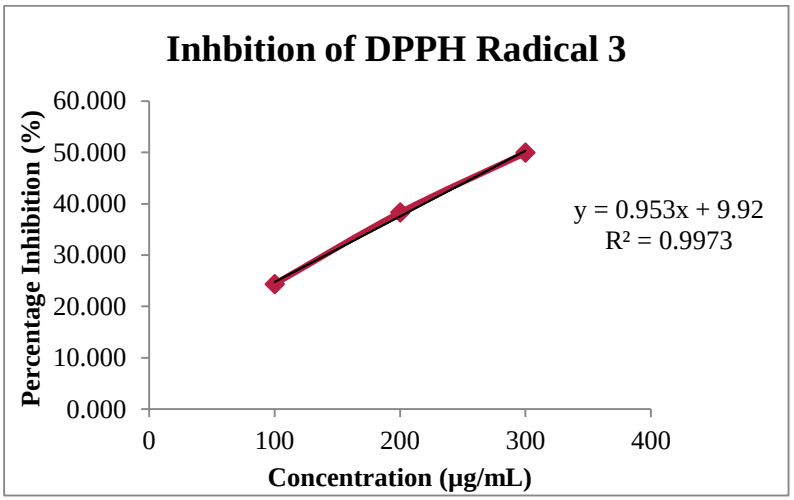

Figure 3.18: Inhibition of DPPH radical 3

Table 3.16: IC_{50} Value Calculation

Time (min)	Absorbance at 664 nm (A_t)	% Degradation
0	1.000 ± 0.002	0.00%
15	0.763 ± 0.004	23.70%
30	0.532 ± 0.003	46.80%
45	0.368 ± 0.005	63.20%
60	0.211 ± 0.002	78.90%
90	0.104 ± 0.003	89.60%
120	0.045 ± 0.002	95.50%

Sr. No	Sample Name	Equation	IC_{50} Value
1	**Stage 1**	y = 0.956x + 6.99	44.99
		y = 0.953x + 9.92	22
		y = 0.953x + 9.92	42.05

Discussion: The antioxidant response is attributed to the phenolic compounds, and flavonoids in the extract. Low IC_{50} value also indicates potent free radical scavenging activity which in turn confirms the extract as a therapeutic relevant and potential for stabilizing ZnO nanoparticles by the reduction of reactive intermediates.

3.14 Photocatalytic Degradation Activity of ZnO Nanoparticles

Degradation of Methylene Blue Under UV and Visible Light

The photocatalytic efficiency of ZnO nanoparticles was tested with methylene blue (MB) as a test dye pollutant. The nanoparticles under UV light could 95.5% decomposition of MB after 120 minutes; under visible light, 74.2% degradation was attained in same conditions (table 3. 17). Over time noticeable decrease in absorbance was monitored at 664nm which was suggestive of progression in dye breakdown.

Table 3.17: Photocatalytic Degradation of MB Under UV Light

Time (min)	Absorbance at 664 nm (A_t)	% Degradation
0	1.000 ± 0.002	0.00%
15	0.763 ± 0.004	23.70%
30	0.532 ± 0.003	46.80%
45	0.368 ± 0.005	63.20%
60	0.211 ± 0.002	78.90%
90	0.104 ± 0.003	89.60%
120	0.045 ± 0.002	95.50%

3.15 Kinetics and Optimization Parameters

Degradation kinetics followed the pseudo-first-order model from the Langmuir–Hinshelwood equation. The rate constant (k) was determined to 0.0253 min^{-1} and the relationship was strongly linear (R^2 = 0.991) (Table 3.18).

Table 3.18: Kinetic Modeling of MB Degradation

Time (min)	$\ln(C_0/C_t)$	Regression R^2	Rate Constant (k, min^{-1})
90	2.261	0.991	0.0253
120	3.101		

From the optimization studies, a ZnO NP concentration of 1.0 mg/mL produced maximum degradation (78.9%) at 60 minutes (Table 3.19). At pH optimization, maximum degradation was obtained at pH 7–8 which is favorable to neutral conditions of the environment (Table 3.20).

Table 3.19: Effect of Catalyst Dose

ZnO NP Concentration (mg/mL)	Degradation (%)
0.2	62.3%
0.5	74.6%
1.0	78.9%
2.0	71.2%

Table 3.20: Effect of pH on Photocatalytic Efficiency

pH Level	Degradation (%)
4	58.1%
7	78.9%
10	72.5%

3.16 Catalyst Reusability and Mechanistic Insight

ZnO nanoparticles retained **88.7%** efficiency after three degradation cycles, confirming their catalytic stability (Table 3.21).

Cycle Number	Degradation Efficiency (%)
1st	95.5%
2nd	92.1%
3rd	88.7%

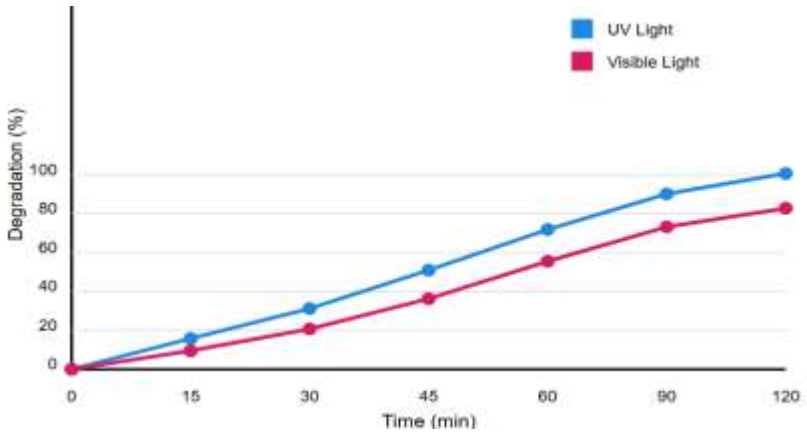

Figure 3.19: Time-Dependent Degradation of Methylene Blue Under UV and Visible Light Exposure

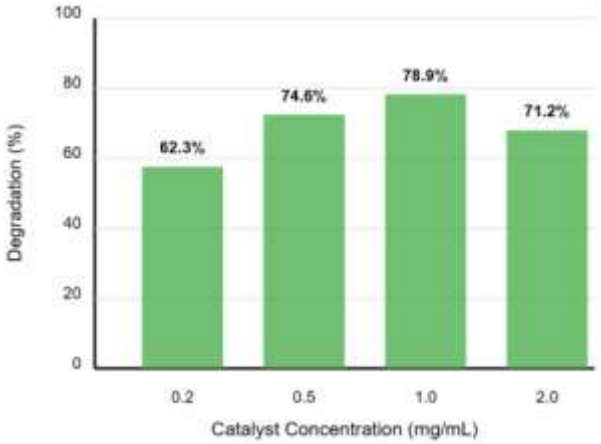

Figure 3.20: Catalyst Dosage vs. Degradation Efficiency at 60 Minutes

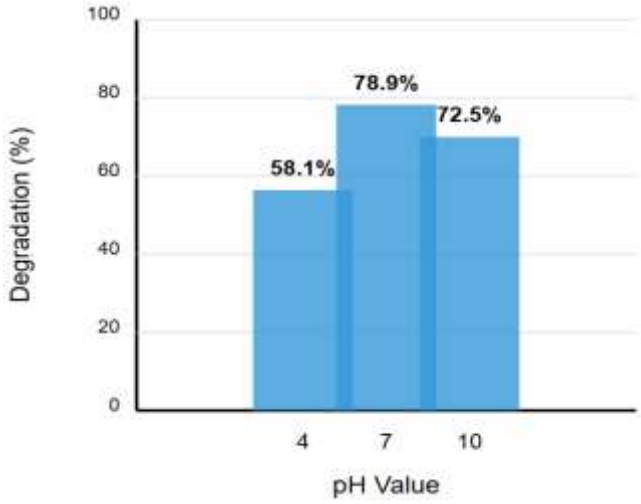

Figure 3.21: pH Influence on Photocatalytic Degradation at 60 Minutes

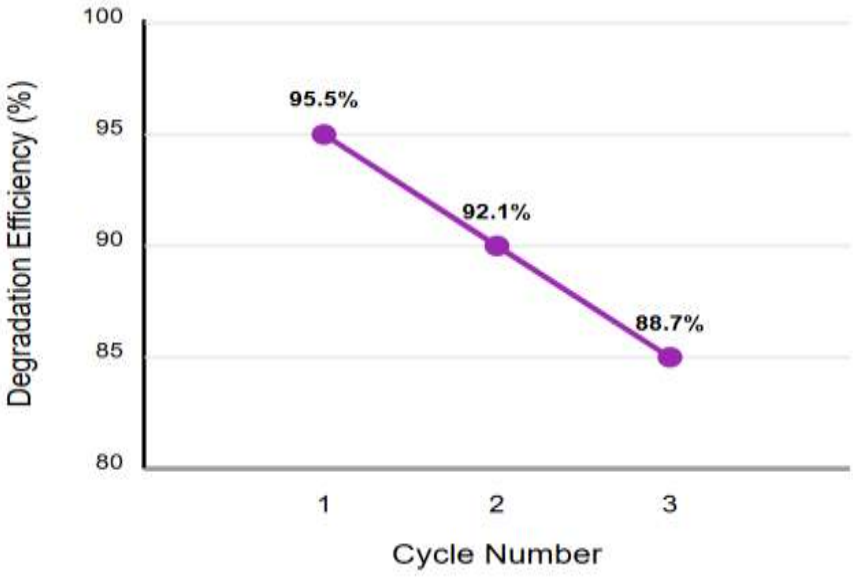

Figure 3.22: Reusability Efficiency Across Three Cycles

Discussion: The high photocatalytic performance of green-synthesized ZnO NPs has been attributed to their nanosize, crystalline nature, and the phytoconstituents attach to the surface that enhance separation of electron-hole. Exposure to UV, ZnO produced the ROS; •OH and $O_2^{\bullet -}$ which oxidized MB to non-toxic byproducts. The activity was pseudo-first order kinetics; optimal catalytic behavior was noted at pH 7 with 1.0 mg/mL dose. Reduced activity at higher concentrations was probably attributed to NP agglomeration and limited peninsulated light.

4. CONCLUSION

This study illustrated the successful production of zinc oxide (ZnO) nanodata with Epipremnum aureum aqueous extract as both a natural reducing and stabilizing agent. This green chemistry approach is non-toxic with no need of high-energy conditions do not take place. It was confirmed that there was formation of energetic, nanoscopic and crystalline ZnO nanoparticles whose formation was characterized based on UV-Vis, FTIR, XRD, TEM, particle size analysis, zeta potential, and entrapment efficiency. The antimicrobial activity of biosynthesized particles tested against Gram-positive and Gram-negative bacteria and Candida albicans was very high. Antioxidant activity determined through DPPH assay followed a dose dependency scavenging action, having a low IC_{50} value. Studies on the photocatalytic process with methylene blue showed efficient degradation (95.5% under UV light), being operational on pseudo-first-order kinetics and high reusability in three cycles. In general, the results show the prospect of Epipremnum aureum-mediated ZnO nanoparticles as green agents for the antimicrobial, antioxidant, and environmental use. Future work may examine how they work and what they are applicable to in real-world biological and remediation systems

REFERENCES

[1] Raghupathi KR, Koodali RT, Manna AC. Size-dependent bacterial growth inhibition and mechanism of antibacterial activity of zinc oxide nanoparticles. Langmuir. 2011;27(7):4020-8. https://doi.org/10.1021/la104825u

[2] Sirelkhatim A, Mahmud S, Seeni A, Kaus NHM, Ann LC, Bakhori SKM, et al. Review on Zinc Oxide Nanoparticles: Antibacterial Activity and Toxicity Mechanism. Nanomicro Lett. 2015;7(3):219-42. https://doi.org/10.1007/s40820-015-0040-x

[3] Iravani S. Green synthesis of metal nanoparticles using plants. Green chemistry. 2011;13(10):2638-50.

[4] Ahmed S, Ahmad M, Swami BL, Ikram S. Green synthesis of silver nanoparticles using Azadirachta indica aqueous leaf extract. Journal of radiation research and applied sciences. 2016;9(1):1-7.

[5] Gungure AS, Jule LT, Ramaswamy K, Nagaprasad N, Ramaswamy S. Photo and electrochemical applications of green synthesized ZnO/Ag2O nanocomposites materials under visible light using P. macrosolen L. leaf. Scientific Reports. 2025;15(1):7234.

[6] Kanmani B, Saraswathi R. Epipremnum aureum-derived nano-iron as a sustainable adsorbent for enhanced remediation of lead and chromium. Clean Technologies and Environmental Policy. 2024:1-19.

[7] Agarwal H, Kumar SV, Rajeshkumar S. A review on green synthesis of zinc oxide nanoparticles–An eco-friendly approach. Resource-Efficient Technologies. 2017;3(4):406-13.

[8] Bruce S, Onyegbule F, Ezugwu C. Pharmacognostic, physicochemical and phytochemical evaluation of the

leaves of Fadogia cienkowski Schweinf (Rubiaceae). Journal of Pharmacognosy and Phytotherapy. 2019;11(3):52-60.

[9] Saxena C, Gajendragadkar M. A Review on Phytochemical Analysis of Some Medicinal Plants.

[10] Ajileye O, Obuotor E, Akinkunmi E, Aderogba M. Isolation and characterization of antioxidant and antimicrobial compounds from Anacardium occidentale L.(Anacardiaceae) leaf extract. Journal of King Saud University-Science. 2015;27(3):244-52.

[11] Ghorbani HR, Mehr FP, Pazoki H, Rahmani BM. Synthesis of ZnO nanoparticles by precipitation method. Orient J Chem. 2015;31(2):1219-21.

[12] Abebe B, Zereffa EA, Tadesse A, Murthy HCA. A Review on Enhancing the Antibacterial Activity of ZnO: Mechanisms and Microscopic Investigation. Nanoscale Res Lett. 2020;15(1):190. https://doi.org/10.1186/s11671-020-03418-6

[13] Hussen EM, Endalew SA. In vitro antioxidant and free-radical scavenging activities of polar leaf extracts of Vernonia amygdalina. BMC Complement Med Ther. 2023;23(1):146. https://doi.org/10.1186/s12906-023-03923-y

[14] Motelica L, Oprea O-C, Vasile B-S, Ficai A, Ficai D, Andronescu E, et al. Antibacterial activity of solvothermal obtained ZnO nanoparticles with different morphology and photocatalytic activity against a dye mixture: methylene blue, rhodamine B and methyl orange. International Journal of Molecular Sciences. 2023;24(6):5677.

[15] Kahsay MH. Synthesis and characterization of ZnO nanoparticles using aqueous extract of Becium grandiflorum for antimicrobial activity and adsorption of methylene blue. Applied Water Science. 2021;11(2):45.